Inverse modeling for characterizing surface water/groundwater exchanges

J.-L. Pinault, Susanne Schomburgk

Inverse modeling for characterizing surface water/groundwater exchanges

J.-L. Pinault[1] and S. Schomburgk[2]

Received 15 September 2005; revised 5 May 2006; accepted 23 May 2006; published 10 August 2006.

[1] Inverse modeling is presented and applied to the computation of groundwater inflow in a shallow aquifer (the Alsace aquifer, west of the Rhine River, France) by separating pressure head variations into three components: recharge from rainfall, and exchanges with surface water in the Rhine River and in tributaries flowing out of the Vosges Mountains. The point estimates are interpolated for the whole aquifer to visualize the proportion of contribution and the response times. To represent the surface water/groundwater exchange, this method uses directly observed data of streamflow, precipitation, and pressure head without requiring either spatial description of the hydrosystem or knowledge of the boundary conditions on both sides of the Rhine (the border between France and Germany). Several zones of the aquifer are shown to be strongly influenced by the hydrographical network where response times are short. Although the direct influence of the Rhine is limited to its immediate surroundings, it contributes to maintaining the low level of the Alsace water table as a whole. The response time of recharge from rainfall closely reflects the thickness of the vadose zone south of Selestat and at the northern end of the Alsace plain whereas it discloses the contours and the thickness of the loess terraces nearby and south of Strasbourg to Selestat.

Citation: Pinault, J.-L., and S. Schomburgk (2006), Inverse modeling for characterizing surface water/groundwater exchanges, *Water Resour. Res.*, *42*, W08414, doi:10.1029/2005WR004587.

1. Introduction

[2] The surface water network of the Alsace plain and its relations with groundwater have been subjected to particular attention, due to both the vulnerability of the hydrosystem and the particularity of the ecosystem [*Carbiener*, 1983; *Trémolières et al.*, 1993, 1994, 1997; *Kaden*, 1994; *Schmitt*, 2001; *Sánchez-Pérez and Trémolières*, 2003].

[3] The Alsace (or Rhine) aquifer in the Quaternary alluvium of the Rhine graben in France is one of Europe's major groundwater resources. Extending from the Rhine River in the east to the Vosges mountains in the west, it contains an estimated 35 km^3 of groundwater and supplies most of the water used for domestic, agricultural, and industrial purposes with 0.35 km^3, which corresponds to 20% of the total groundwater output. The shallow aquifer creates typical landscapes, the so-called Alsacian "rieds" (from the reeds that typically grow there) and wetlands. Poorly protected by permeable cover sediments, it is particularly vulnerable to both point-source and nonpoint-source pollution of agricultural or industrial origin, including salt water and brines produced by former potash mines. The groundwater level is affected by (1) recharge from rainfall, (2) lateral inflow by infiltration in the Vosges mountains, (3) exchanges with the surface water network recharging or draining the aquifer, and (4) pumping for domestic, industrial, or agricultural needs. Water table fluctuations have consequences on the landscape and on human activities: drying up of wetlands, groundwater-induced floods, and the propagation of pollution.

[4] We propose a method for characterizing water table variations by separating the fluctuations of groundwater head into components associated with recharge from rainfall and exchanges with the surface water network, and by estimating response times. Parametric impulse responses are computed at piezometer locations in order to quantify the contribution of each component and the mean transfer times. Kriging is used to extend the point estimates to the entire aquifer.

[5] Contrary to meshed models, this method does not require either spatial description of the hydrosystem or knowledge of the boundary conditions on both sides of the Rhine (the border between France and Germany) since head variation separation is done point by point before kriging, without any notion of spatial continuity. This new approach improves and updates our knowledge of the Alsace aquifer west of the Rhine, a regional hydrodynamic model of which has been developed for water resource management.

2. Field Description

[6] The Alsace aquifer is contained in the alluvia deposited by the Rhine and its tributaries during the Pliocene and the Quaternary in the Rhine graben (Figure 1). It extends over approximately 3040 km^2. The alluvia of the Alsace plain include (1) Rhine sands and clay deposits mostly with

[1]Water Research Division, Bureau de Recherches Géologiques et Minières, Orléans, France.
[2]Bureau de Recherches Géologiques et Minières, Strasbourg, France.

0043-1397/06/2005WR004587

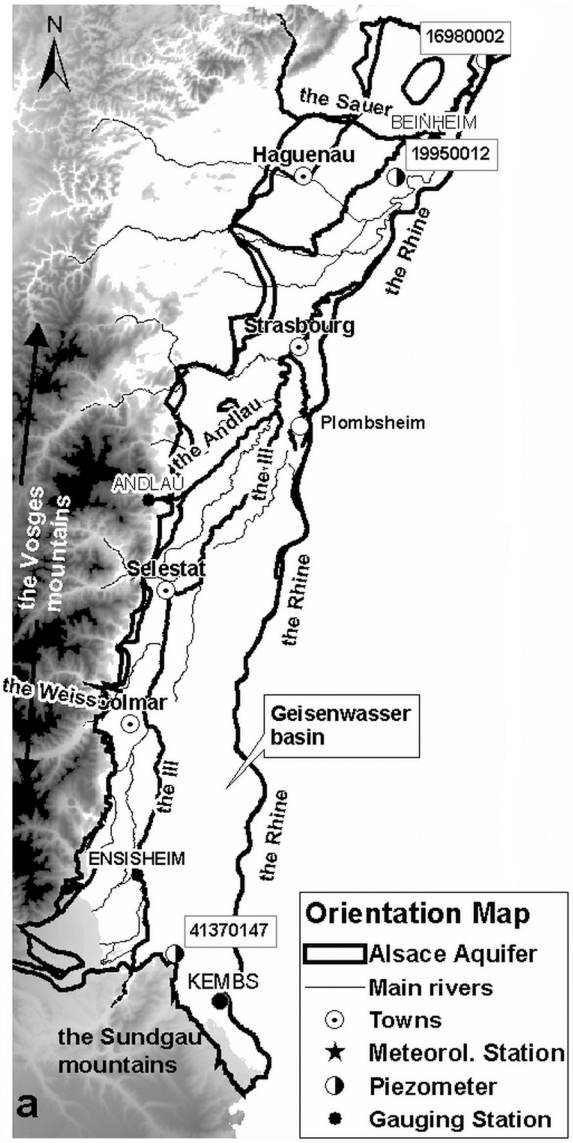

Figure 1. Map of the Alsace region.

material from the Alps; (2) alluvial cones of the Vosgian rivers; and (3) Pliocene alluvia in the Haguenau area. These gravel-sand alluvia, with some clay intercalations, are permeable, especially the Rhine alluvia. The thickness varies from a few meters on the edges to an average of 70 m, and can reach up to 200–250 m in some depocenters such as the Geiswasser Basin. The substratum is constituted of low permeable marls.

[7] Different strata can be distinguished in the alluvium according to hydraulic characteristics and lithologic composition. The recent alluvia near the surface are generally fresh and permeable, whereas the older, deeper alluvia are more or less weathered, more silty, and generally less permeable. These strata are separated in places by clay and fine sand layers. These intercalations can locally constitute hydraulic barriers that prevent vertical circulation and protect deep groundwater from surface pollution. The vertical circulation velocity and response time allow to estimate the risk of point-source and nonpoint-source pollution. The zones characterized by long response times are around Strasbourg where large areas are covered by a thick layer of fine, low permeable loess, and in the west, in the middle of Alsace, where the vadose zone is relatively thick.

[8] Southern Alsace is influenced mainly by leakage from rivers (i.e., the Ill river and small rivers flowing out of the mountains in the south of the study zone) and canals (such as the Hardt canal, used for irrigation). These surface waters contribute significantly to the water flux collected by the aquifer.

[9] The circulation velocity of groundwater from south to north in the Rhine graben is only 1–2 m/d on average due to a low slope of around 0.1%. Groundwater flows to the east or northeast only near the Vosges.

[10] The thickness of the vadose zone varies between a few tens of centimeters to more than 10 m in the Hardt area. In the rieds, the groundwater is close to the surface and upwells in artesian springs. The water table varies, in general, 1–3 m/yr.

[11] The climate of the Alsace plain is continental, with low rainfall in the central part (600 mm/yr). The Vosges mountains are characterized by a stronger influence of the oceanic climate, mean annual rainfall reaching 2300 mm in the High Vosges. The groundwater is recharged by (1) Vosgian rivers around their outlets in the plain, (2) canals partly supplied with the Rhine in the southern, upper Rhine valley, and (3) rainfall on all surfaces through the silt and layers of loess. Nevertheless, the functioning of the Alsace aquifer is controlled mainly by exchanges with the surface water network, the rivers downstream from Colmar both recharging and draining the groundwater. Rainfall does not contribute more than 15–20% on average to the recharge. The surface area of the Rhine catchment at the input of the Alsace plain is 37,000 km^2. The Rhine flow depends mainly on the melting of the alpine glaciers, and the water level can be low in the winter. High water levels are generally observed in the winter or spring and flow is maintained in summer. Vosgian river flow is controlled by snowmelt and rainfall in the Vosges mountains, and flooding occurs in winter.

3. Mathematical Modeling and Numerical Analysis

[12] A general method consists of developing inverse models where the quintessential problem is determining conductivity from observations of hydraulic head. This is usually achieved through systematic fitting of parameter values to match measured values [*Carrera and Neuman*, 1986; *Cooley et al.*, 1986; *Yeh*, 1986; *Carrera*, 1987; *Ginn and Cushman*, 1990; *Sun*, 1994; *Kitanidis*, 1995, 1999; *Ramarao et al.*, 1995; *Lavenue et al.*, 1995; *McLaughlin and Townley*, 1996].

[13] The approach presented here separates spatial coordinates and time [*Pinault*, 2001; *Pinault et al.*, 2001a, 2001b, 2004, 2005]. Instead of estimating conductivity according to spatial coordinates, which uses regularization techniques to obtain a regular solution, each piezometer is processed independently and the piezometric levels are separated into components according to time. The number of components is set from the inputs of the inverse models, provided they can be decorrelated, which presupposes that the cross correlogram obtained from every pair of input

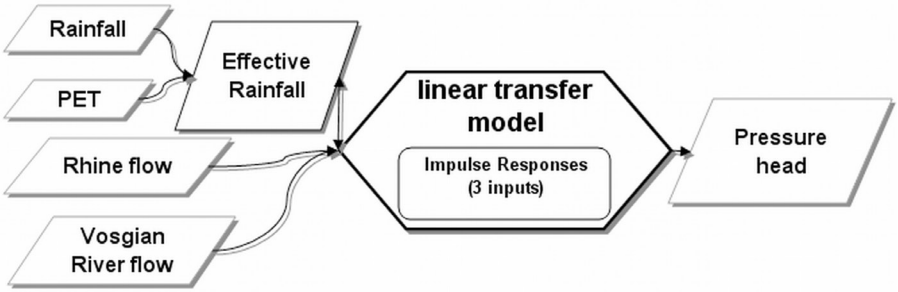

Figure 2. The transfer model used to separate pressure head variations into three components: (a) recharge from rainfall, (b) exchange with the Rhine, and (c) exchanges with the Vosgian surface water network. Input and output variables are dimensionless (divided by their standard deviation). Gray boxes refer to measured data.

signals is lower than 0.75, whatever the lag. Nevertheless, this condition is not sufficient and the impulse responses must be as short as possible. Indeed, the components that are used are effective rainfall and streamflow. The longer the impulse responses, the more correlated the inputs appear, since long-term correlation is unavoidable due to the influence of rainfall on streamflow.

[14] The Alsace aquifer head variations can be separated into three components: (1) recharge from rainfall, (2) exchanges with the Rhine River, and (3) exchanges with the Vosgian tributaries. To make head variation separation reliable, a parametric model is used as impulse responses, which decreases the number of degrees of freedom of the inverse model. Piezometric series are selected so that there are enough observation years to be representative of low and high groundwater level conditions, i.e., at least 10 years.

3.1. Transfer Model Architecture

[15] The transfer model architecture is shown in Figure 2. It is relating three inputs (effective rainfall, flow in the Rhine River, and flow in Vosgian drainages) to the variation in pressure head in piezometers. The relationship between the inputs and outputs is based on impulse response functions, the parameters of which are obtained through the inversion, i.e., the minimization of the quadratic form

$$\sum_{i=1,N} \left(\Delta H_{\mathrm{obs}}(t_i) - \Delta H_{mod}(t_i)\right)^2$$

where ΔH_{obs} and ΔH_{mod} are the observed and the modeled pressure head variations.

[16] Exchanges between the groundwater around a piezometer and a stream can be considered as proportional to the water level in the stream, regardless of the direction and the absolute value of the hydraulic gradient since variations in water level in the stream are much faster than groundwater level variations. The variables used as input and output in the inverse models are dimensionless; they are divided by their standard deviation. Water level in the stream can therefore be replaced by streamflow if the water level and streamflow are proportional, which is generally the case within a large variation interval of river bank water level. Biases are often observed for low or high water levels, when the gauging curves deviate from the linearity, but they have little effect on the results. Since input and output variables are reduced to unit standard deviation, inverse models are robust (streamflows fulfill the equation of continuity) and insensitive to mean rainfall in particular places of the basin. Short-term rainfall variations, however, have a strong influence on the transfer model outputs.

[17] The mathematical development is based on that of *Pinault et al.* [2001a, 2001b, 2005]. Considering the flow $Q_1(t)$ of the Rhine and the flow $Q_2(t)$ of a Vosgian stream considered as representative of the surface water network, the following relationship can be written

$$\Delta \mathrm{H}(t) = \lambda.\boldsymbol{\Gamma} * \mathbf{R}_{eff} + \lambda_1.\boldsymbol{\Gamma}_1 * \mathbf{Q}_1 + \lambda_2.\boldsymbol{\Gamma}_2 * \mathbf{Q}_2 + \varepsilon, \qquad (1)$$

where the asterisk represents the discrete convolution product; $\Delta \mathrm{H}(t)$ is the piezometric level expressed in relation to the low groundwater level; $\boldsymbol{\Gamma}$, $\boldsymbol{\Gamma}_1$, $\boldsymbol{\Gamma}_2$ are normalized impulse responses (the area being unity): $\boldsymbol{\Gamma}$ is the transfer function of effective rainfall $\mathbf{R}_{eff}$ into the aquifer, and $\boldsymbol{\Gamma}_1$ and $\boldsymbol{\Gamma}_2$ are transfer functions related to flows $\mathbf{Q}_1$ and $\mathbf{Q}_2$; they express recharge and drainage of the aquifer by the streams. The variables $\Delta \mathrm{H}(t)$, $\mathbf{R}_{eff}$, $\mathbf{Q}_1$, and $\mathbf{Q}_2$ are reduced to unit standard deviation.

[18] The λ, λ_1, and λ_2 are positive factors related by the relationship

$$\lambda \overline{R_{eff}}/\overline{\Delta \mathrm{H}} + \lambda_1 \overline{Q_1}/\overline{\Delta \mathrm{H}} + \lambda_2 \overline{Q_2}/\overline{\Delta \mathrm{H}} = 1, \qquad (2)$$

which expresses water mass conservation. The terms $\lambda.\mathbf{R}_{eff}$, $\lambda_1\mathbf{Q}_1$, and $\lambda_2\mathbf{Q}_2$ represent the contribution of rainfall and streams to the water flux collected by the aquifer. The random part, ε, the mean of which is zero, represents erratic, complex, and usually short term variability of the pressure head that is not explained by the model, including measurement errors, and whether they are due to instrumentation or sampling defects.

3.2. Parametric Impulse Responses

[19] Impulse responses $\boldsymbol{\Gamma}$, $\boldsymbol{\Gamma}_1$, $\boldsymbol{\Gamma}_2$ are defined on the interval $[0,\tau]$ so that

$$\begin{cases} \Gamma(t_i) = A \exp\left(-\ln(2)(t_i - T)^2/D^2\right) * \exp(-t_i \ln(2)/L) \\ \qquad \text{if } 0 \le t_i \le \tau \\ \Gamma(t_i) = 0 \quad \text{elsewhere} \end{cases} . \qquad (3)$$

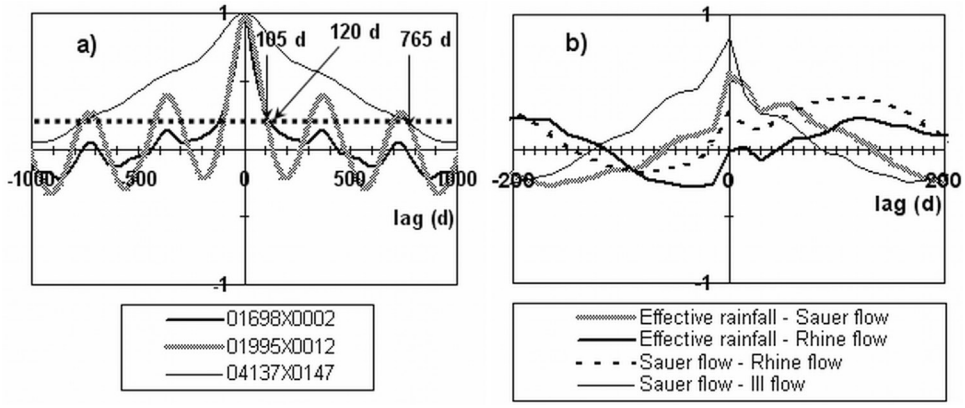

Figure 3. (a) Autocorrelograms of pressure heads measured at three piezometers. The regulation times of pressure heads are defined from the intersection of their autocorrelograms with the dotted line $y = 0.2$ as indicated by the arrows. (b) Cross correlograms of some variables used as inputs in the inverse models.

This model is the expression of the recharge represented by the Gaussian $\exp(-\ln(2)(t_i - T)^2/D^2)$ to take into account dispersive effects leading to the broadening of impulse responses, followed by its discharge represented by the exponential law $\exp(-t_i \ln(2)/L)$ to take into account the recession. Parameter T represents the delay of the recharge process after a rainfall event or a flow impulse, depending on the impulse response, D represents the duration of the recharge, L is the recession constant, and A is the normalization constant. The succession of these two phenomena is the convolution product of the recharge law by the discharge law. Because of its small number of degrees of freedom (three per impulse response), this parametric model does not need any regularization technique to be calibrated: The small number of degrees of freedom as well as the water mass conservation (2) make that the equation (1) is invertible.

3.3. Reference Level of Piezometers

[20] For each piezometer, the reference level $\mathbf{H}^0$ from which are expressed the hydraulic head variations $\Delta\mathbf{H} = \mathbf{H} - \mathbf{H}^0$ corresponds to the low groundwater level. This reference level is estimated so that

$$\mathbf{H}^0 = m - \beta\sigma, \tag{4}$$

where m and σ are the mean and the standard deviation of $\mathbf{H}$, respectively. The parameter β takes the value 2.5 when the regulation time of the piezometric level $\mathbf{H}$ is less than 1 year, which corresponds to a 160-year return period of $\mathbf{H}^0$ provided $\mathbf{H}$ follows a Gaussian distribution. The β takes the value 3.95 when the regulation time is 2 years, the return period being 160^2 years if the climatic conditions of two successive years can be considered as independent. The actual value of β is interpolated from the actual value of the regulation time of $\mathbf{H}$, which is estimated from the $\mathbf{H}$ autocorrelogram (Figure 3a).

3.4. Calculation of Effective Rainfall From Rainfall and Potential Evapotranspiration (PET)

[21] The mean effective rainfall $\overline{\mathrm{R}}_{eff}$ is such that

$$\overline{\mathrm{R}}_{eff} = \gamma\,\overline{\mathrm{R}}, \tag{5}$$

where γ is the proportion of rainwater lost by evapotranspiration, i.e., the mean contribution of rainfall to effective rainfall whose value oscillates around 0.45 depending on the piezometer.

[22] Effective rainfall R_{eff} is calculated from rainfall R and the effective rainfall threshold Ω, such that

$$\mathrm{R}_{eff}(t_i) = \begin{cases} \mathrm{R}(t_i) - \Omega(t_i) & \text{if } \mathrm{R}(t_i) \geq \Omega(t_i) \\ 0 & \text{if } \mathrm{R}(t_i) < \Omega(t_i) \end{cases}. \tag{6}$$

The effective rainfall threshold $\Omega(t_i)$ is related to both rainfall and potential evapotranspiration, such that

$$\mathbf{\Omega} = \mathbf{\Gamma}_{\Omega,PET} * \mathbf{PET} + \mathbf{\Gamma}_{\Omega,R} * \mathbf{R} + \mathrm{C}^{\mathrm{st}}, \tag{7}$$

where $\mathbf{\Gamma}_{\Omega,PET}$ and $\mathbf{\Gamma}_{\Omega,R}$ are impulse responses of $\mathbf{\Omega}$ to potential evapotranspiration **PET** and to rainfall **R**, respectively. These impulse responses are represented by trapezes with four degrees of freedom, with $\mathbf{\Gamma}_{\Omega,PET}$ being positive, $\mathbf{\Gamma}_{\Omega,R}$ being negative; rainfall induces a decrease in $\mathbf{\Omega}$, whereas potential evapotranspiration produces an increase in $\mathbf{\Omega}$. The impulse responses and the constant C^{st} are obtained in the inverse method.

3.5. Regionalization of Rainfall at the Basin Scale

[23] Rainfall data from several weather stations are therefore used in order to reveal pluviometers whose short-term

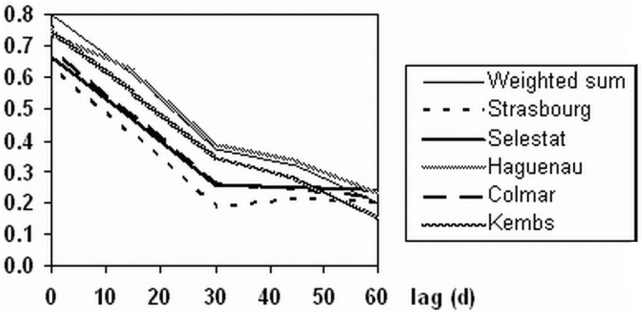

Figure 4. Cross correlograms between the Ill flow at Ensisheim and effective rainfalls.

Table 1. Representation of the Contribution of Rainfall Data Measured at Rain Stations to the Weighted Sums R_Σ Estimated From Vosgian River Flows[a]

	Catchment Area, km^2	Distance From Kembs, km	Weight Associated to Rain Stations				
			Kembs (Mulhouse)	Colmar	Selestat	Strasbourg	Haguenau
Doller (Reiningue)	180	25	0.21	...	0.30	...	0.49
Ill (Ensisheim)	1038	31	0.44	0.09	0.22		0.25
Ill (Colmar)	1784	55	0.40	0.08	0.25		0.27
Fecht (Ostheim)	447	62	0.29	...	0.33	...	0.38
Weiss (Kaysersberg)	117	64	0.23	...	0.36	...	0.41
Giessen (Selestat)	260	73	0.13	...	0.41	...	0.46
Andlau (Andlau)	42	86	0.10	...	0.37	...	0.53
Sauer (Beinheim)	541	145	0.03	0.12	0.08	...	0.77

[a]Ten years are used for calculations. The weights associated to the Ill River are almost the same because 58% of streamflow at Colmar comes from Ensisheim. The Strasbourg station never contributes to the weighted sums, and the weights associated to Colmar are low. The only stations whose weight is significant are Kembs, Selestat, and Haguenau, the contribution of which seems not related to the location of gauging stations.

fluctuations are correlated with Vosgian river flows. A sum R_Σ of rainfall series is defined so as to optimize the contribution of each pluviometer to the transfer models. For every model of which the output is a Vosgian river flow Q, the cross correlogram $\mathrm{Cor}_{R_\Sigma,Q}(\tau)$ of R_Σ and the output is maximized. From the weighted sum,

$$R_\Sigma = \sum_{k=1,p} \delta_k \, R_k \qquad \delta_k \geq 0 \; k = 1, \cdots, p \qquad \sum_{k=1,p} \delta_k = 1 \quad (8)$$

(p being the number of pluviometers), the cross correlogram $\mathrm{Cor}_{R_\Sigma,Q}(\tau)$ of R_Σ and the output of the transfer model can be written as

$$\mathrm{Cor}_{R_\Sigma,Q}(\tau) = \frac{\sum_{i=1,N} \left[R_\Sigma(t_i) - \overline{R_\Sigma}\right]\left[Q(t_i+\tau) - \overline{Q}\right]}{\sqrt{\sum_{i=1,N} \left[R_\Sigma(t_i) - \overline{R_\Sigma}\right]^2} \sqrt{\sum_{i=1,N} \left[Q(t_i) - \overline{Q}\right]^2}}, \quad (9)$$

where $\overline{R_\Sigma}$ and $\overline{Q}$ are the mean of $R_\Sigma(t_i)$ and $Q(t_i)$, respectively (N being the number of sampling steps).

[24] The weighting factors δ_k are calculated so that they maximize the objective function:

$$O_\Sigma = \sum_{l=1,S} \mathrm{Cor}_{R_\Sigma,Q}(\tau_l) \quad (10)$$

defined from the cross correlogram $\mathrm{Cor}_{R_\Sigma,Q}(\tau_l)$ for small lags (Table 1, Figure 4).

[25] The higher the objective function O_Σ, the stronger the causal relationship between the weighted rainfall series R_Σ reduced to unit standard deviation and the output Q and, consequently, the more representative the combination of pluviometers.

[26] As observed by *Pinault et al.* [2005], although the mean rainfall significantly varies onto the basin (there are strong gradients from the mountains into the plain), the weighted rainfall series R_Σ are strongly correlated at the catchment scale with a 15-day time step (Figure 5). Indeed, the weighted sums depend little on the location and the reduced rainfall can be considered as homogeneous at broad scale. In other words, all the linear combinations proposed in Table 1 should be considered as equivalent regardless of the location.

[27] Potential evapotranspiration is obtained from the Colmar weather station. The addition of other stations does not improve the accuracy of the models.

3.6. Data Processing

[28] For each piezometer, the inverse method aims to calculate the impulse responses $\mathbf{\Gamma}$, $\mathbf{\Gamma}_1$, $\mathbf{\Gamma}_2$, $\mathbf{\Gamma}_{\Omega,PET}$, $\mathbf{\Gamma}_{\Omega,R}$, the constant C^{st}, and the factors λ, λ_1, and λ_2, which represent 20 degrees of freedom. From a numerical point of view, the problem is well posed and the solution may be considered unique. No regularization method is therefore needed for inversion. Indeed, regularization techniques in ill-posed problems are required to select the most likely solutions that are the smoothest solutions according to the parsimony principle. In the present inverse model, the solutions are smooth by construction since they are defined from parametric models, whether it is question of transfer functions (3) or impulse responses of $\mathbf{\Omega}$ to potential evapotranspiration **PET** and to rainfall $\mathbf{R}_\Sigma$.

[29] Data processing is done using the TEMPO code [*Pinault*, 2001]. Modeling is done with a 15-day sampling rate (all series are aggregated over contiguous 15-day

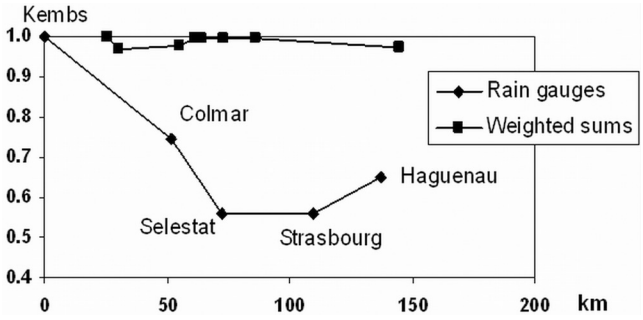

Figure 5. Correlation distance of rainfall. The abscissa represents the scale spacing along a curve line starting from Kembs passing by Colmar and joining Haguenau. Small variations in the correlation coefficients of the weighted sums are not significant, maybe except a slight north-south trend, whereas the correlation coefficients of rainfall data measured at weather stations decrease drastically. Thus disagreements between reduced rainfall data measured at rain stations are mainly due to the noise since the weighted sums turn out to be homogeneous at broad scale.

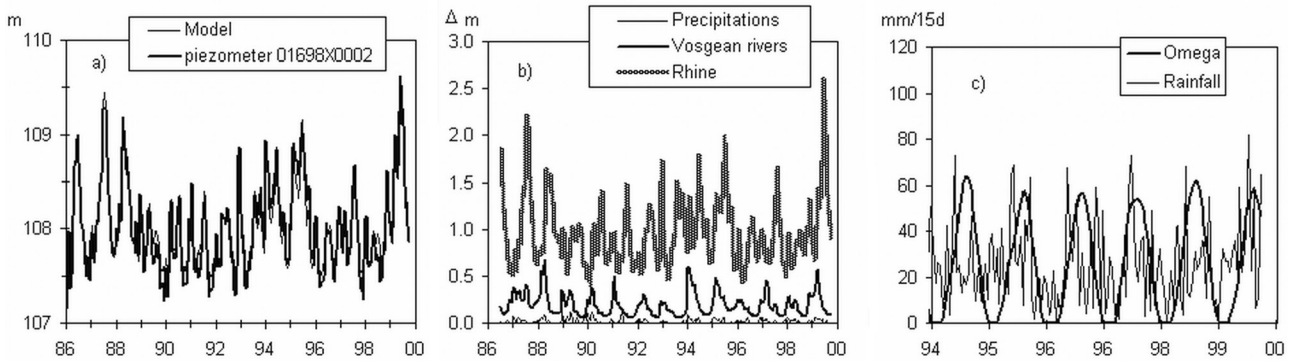

Figure 6. Inverse modeling of groundwater recharge (piezometer 01698X0002 influenced by the Rhine) with a sampling step of 15 days. The variables are expressed in their initial units. (a) Comparison of observed and modeled pressure heads. The Nash coefficient is 0.93. (b) The components of the piezometric variations above the reference level (106.34 m). (c) The effective rainfall threshold $\Omega(t_i)$; 42.2% of total rainfall contributes to groundwater.

periods), which minimizes discrepancies between the models and observations.

[30] The separation of head variations leads to the estimation of the three weights $\lambda.\overline{R_{eff}}/\overline{\Delta H}$, $\lambda_1\overline{Q_1}/\overline{\Delta H}$, and $\lambda_2\overline{Q_2}/\overline{\Delta H}$, the sum of which is 1 from (2). The weights represent the mean contribution of rainfall and streams to head variations. The associated mean response times are the expected value of the lag τ, i.e.,

$$\overline{\tau} = \delta t \sum_{i=0,1,\ldots,N} i\Gamma(i\delta t)$$

where δt is the sampling step, Γ is the corresponding impulse response the order of which is N.

[31] The cross correlograms of variables used as inputs of the inverse models (Figure 3) show that the Rhine flow at the entrance to the Alsace plain (Kembs gauging station) is not influenced by rainfall on the basin. Since the surface area of the Alsace plain is only 8% of that of the Rhine catchment upstream, Rhine flow can be considered to be independent of the effective rainfall in the plain. It is, however, strongly influenced by rainfall in the Alps and snowmelt, hence the high flow in summer. The Vosgian river flows are much more influenced by rainfall on the Alsace plain. Heavy rainfall events are followed by peak flow in all rivers after a 1- or 2-day delay. However, the cross correlograms do not exceed 0.5 since Vosgian river flow depends strongly on the type of rainfall upstream, which differs from that in the Alsace plain due to both the altitude and the climatic barrier created by the Vosges mountains. Effective rainfall and Vosgian river flow can therefore be separated in the inversion process. On the other hand, the Vosgian rivers are much too intercorrelated to be treated independently. Their cross correlogram exceeds 0.8. Only one of them must be selected at the input of the models to represent exchanges between surface water and groundwater. There are many Vosgian rivers, and their flow reflects the geology of the formations they drain and rainfall in the Vosges mountains. Various rivers are therefore selected depending on the location of the piezometers: from north to south, the Sauer at Beinheim, the Andlau at Andlau, the Weiss at Kaysersberg, and the Ill at Ensisheim.

[32] Data processing of three piezometers is explained to show how the effect of rainfall and exchanges with surface water can be characterized: piezometer 01698X0002 influenced mainly by the Rhine, piezometer 01995X0012 influenced by Vosgian rivers, and piezometer 04137X0147 representative of the confined area of the Alsace aquifer.

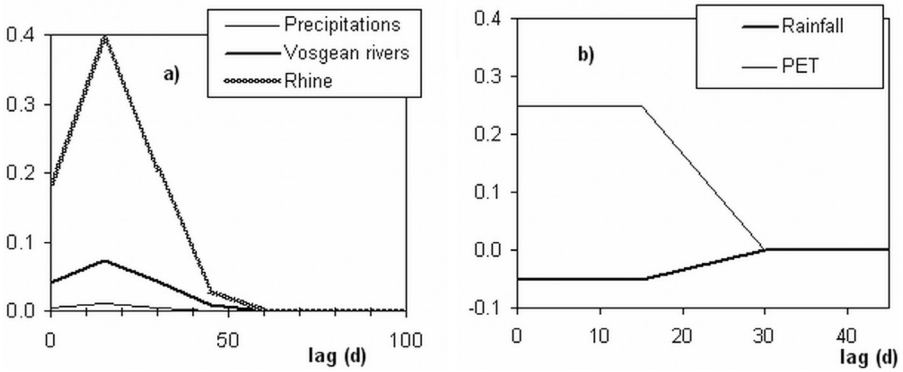

Figure 7. Piezometer 01698X0002. a) Impulse responses $\mathbf{\Gamma}$, $\mathbf{\Gamma}_1$, $\mathbf{\Gamma}_2$ relative to precipitations and exchanges with Vosgian rivers and Rhine. (b) Impulse responses of the effective rainfall threshold $\mathbf{\Omega}$ to rainfall and potential evapotranspiration (PET).

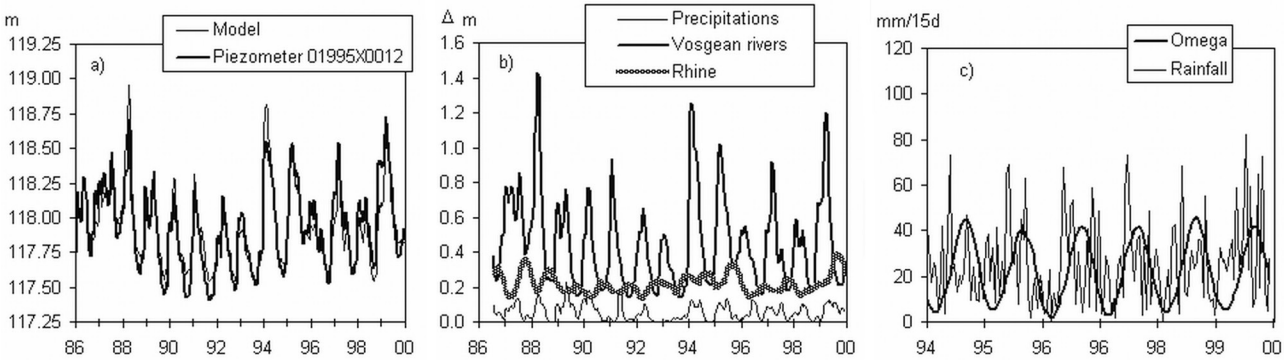

Figure 8. Inverse modeling of groundwater recharge (piezometer 01995X0012 influenced by the Vosgian rivers). (a) Comparison of observed and modeled pressure heads. The Nash coefficient is 0.86. (b) The components of the piezometric variations above the reference level (117.18 m). (c) The effective rainfall threshold $\Omega(t_i)$; 37.6% of total rainfall contributes to groundwater.

3.7. Piezometer 01698X0002 (Lauterbourg, Northern End of the Alsace Plain) Influenced by the Rhine

[33] Data processing is represented in Figure 6. The Sauer at Beinheim is used to represent the Vosgian rivers. Figure 6c shows the effective rainfall threshold $\mathbf{\Omega}$ used to calculate effective rainfall from the combined rainfall $\mathbf{R}_\Sigma$ (6). This threshold represents both the available soil-storage deficit and the proportion of rainfall that runs off toward the surface water network. It is close to zero in winter when most of the rainfall contributes to groundwater recharge. Impulse responses are short (Figure 7a). Response times to the aquifer are 15.3 days for rainfall, 16.8 days for Vosgian rivers, and 16.5 days for the Rhine. The mean contributions are 1.9%, 16.6%, and 81.5%, respectively. At this location, the water table closely follows the level of the Rhine. Indeed, the Rhine maintains the low groundwater level during the summer. The symmetry of the rapid increase and decrease of impulse responses to surface water flow variations shows that groundwater is either drained or recharged by the surface water network. The rainfall contribution is negligible.

3.8. Piezometer 01995X0012 (Northern End of the Alsace Plain) Influenced by the Vosgian Rivers

[34] Data processing is represented in Figure 8. The Sauer at Beinheim is also used to represent the Vosgian rivers. The groundwater near piezometer 01995X0012 in the north of the Alsace Plain is strongly influenced by the Vosgian rivers, although the low groundwater level is maintained by the Rhine flow during the summer (Figure 8b). Response times to the aquifer are 34 days for rainfall, 25 days for Vosgian rivers, and 93 days for the Rhine (Figure 9a). The mean contributions are 7.6%, 64.9%, and 27.5%, respectively. The rainfall contribution is low compared with exchanges with the surface water network. The rapid increase in the impulse response relative to the Sauer flow indicates the short delay between peak flow and the pressure head increase, whereas drainage is more delayed.

3.9. Piezometer 04137X0147 (Rixheim, Southern End of the Alsace Plain) Representative of the Confined Part of the Alsace Aquifer

[35] Data processing is represented in Figure 10. The Ill at Ensisheim is used to represent the Vosgian rivers. Response times to the aquifer are long, 182 days for rainfall, 361 days for surface water (Figure 11a), which characterizes the behavior of either confined or unconfined groundwater in a poorly transmissive aquifer. Indeed, response times show that both the vadose and saturated zones have low transmissivity at this location where the vadose zone is over 20 m thick. The aquifer is recharged by rainfall and the Vosgian rivers, the Rhine contribution being insignificant.

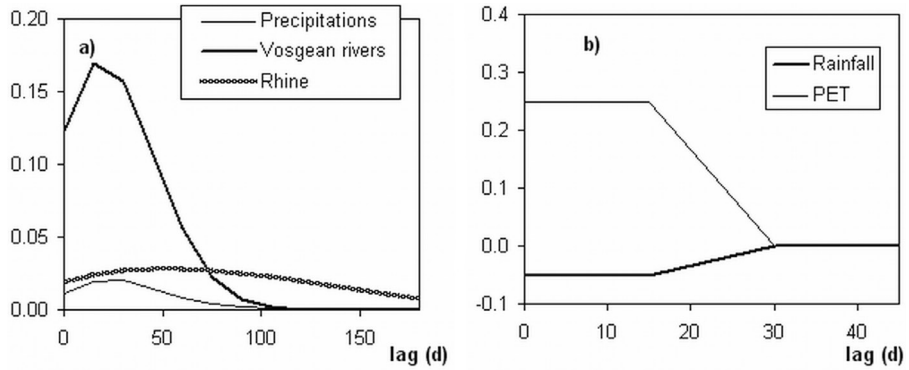

Figure 9. Piezometer 01995X0012. (a) Impulse responses $\mathbf{\Gamma}$, $\mathbf{\Gamma}_1$, $\mathbf{\Gamma}_2$ relative to precipitations and exchanges with Vosgian rivers and Rhine. (b) Impulse responses of the effective rainfall threshold $\mathbf{\Omega}$ to rainfall and PET.

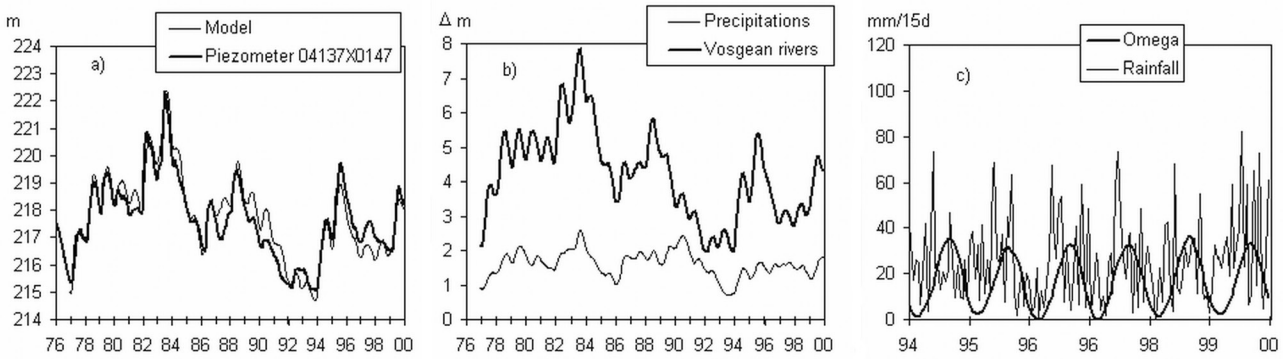

Figure 10. Inverse modeling of groundwater recharge (piezometer 04137X0147 representative of the confined part of the aquifer). (a) Comparison of observed and modeled pressure heads. The Nash coefficient is 0.88. (b) The components of the piezometric variations above the reference level (211.95 m). Contribution of the Rhine is zero. (c) The effective rainfall threshold $\Omega(t_i)$; 52.9% of total rainfall contributes to groundwater.

The mean contributions are 12.0% for rainfall, 87.5% for Vosgian rivers, and 0.5% for the Rhine. The asymmetry of impulse responses reveals a recharging of the aquifer by the surface water network, whereas groundwater discharge is much slower, which suggests that the latter is controlled by regional groundwater flow. The impulse responses of the effective rainfall threshold $\boldsymbol{\Omega}$ to rainfall and PET represented in Figure 7b, Figure 9b, and Figure 11b are similar among the three examples.

3.10. Kriging of the Mean Contributions and Mean Response Times

[36] Figure 12 represents the mean contribution of rainfall and the influence of the surface water network on groundwater. Mean transfer times are presented in Figure 13. Interpolation is done by kriging from 180 piezometers that are not strongly influenced by pumping, hence there is a density of one piezometer per 16 km^2. Indeed, there are nearly 200 piezometers in the Alsace aquifer, some of which have been functioning since 1950. The sampling rate varies between 1 day and 1 week.

[37] The variograms of the mean contributions and mean response times are shown in Figure 14. Only the variograms related to the recharge from rainfall exhibit a nugget effect (Figure 14a and 14d), which discloses the short-scale variability of the vadose zone transmissivity. The correlation range does not overreach 5–7 km in all cases with two exceptions:

[38] 1. The correlation distance of the contribution of the Rhine to the recharge vanishes rapidly and the mean variogram exhibits oscillations (Figure 14b) because the influence of the Rhine on groundwater decreases as we move away from the river bed. This influence is enhanced within a strip along the Rhine, the spatial structure of which is complex depending on the geometry of alluvial deposits.

[39] 2. The correlation distance of the influence of the Vosgian rivers on the water table reaches 20 km (Figure 14c), which is in relation with the pseudoperiodical distribution of these rivers that form a dense network in the foothills of the Vosges.

[40] The spatial representation of the goodness of fit of the pressure head is shown in Figure 15 from the R^2 coefficient:

$$R^2 = \sum_{i=1,N} \left(\Delta H_{\mathrm{obs}}(t_i) - \Delta H_{\mathrm{mod}}(t_i)\right)^2 \Big/ \sum_{i=1,N} \left(\Delta H_{\mathrm{obs}}(t_i) + \Delta H_{\mathrm{mod}}(t_i)\right)^2, \quad (11)$$

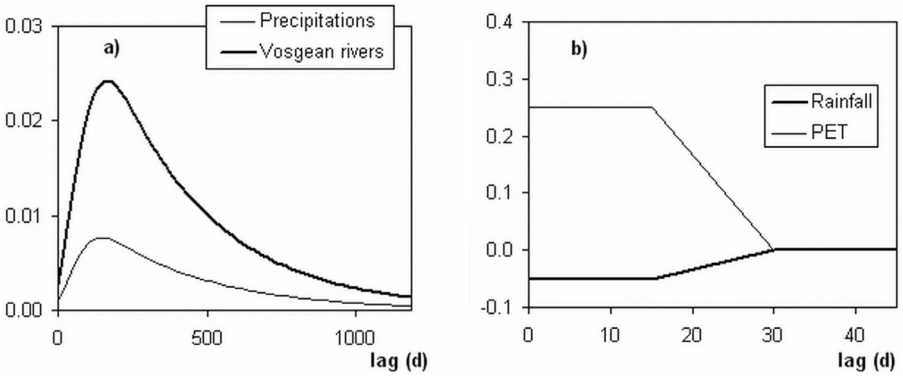

Figure 11. Piezometer 04137X0147. (a) Impulse responses $\boldsymbol{\Gamma}$, $\boldsymbol{\Gamma}_1$ relative to precipitations and exchanges with Vosgian rivers. (b) Impulse responses of the effective rainfall threshold $\boldsymbol{\Omega}$ to rainfall and PET.

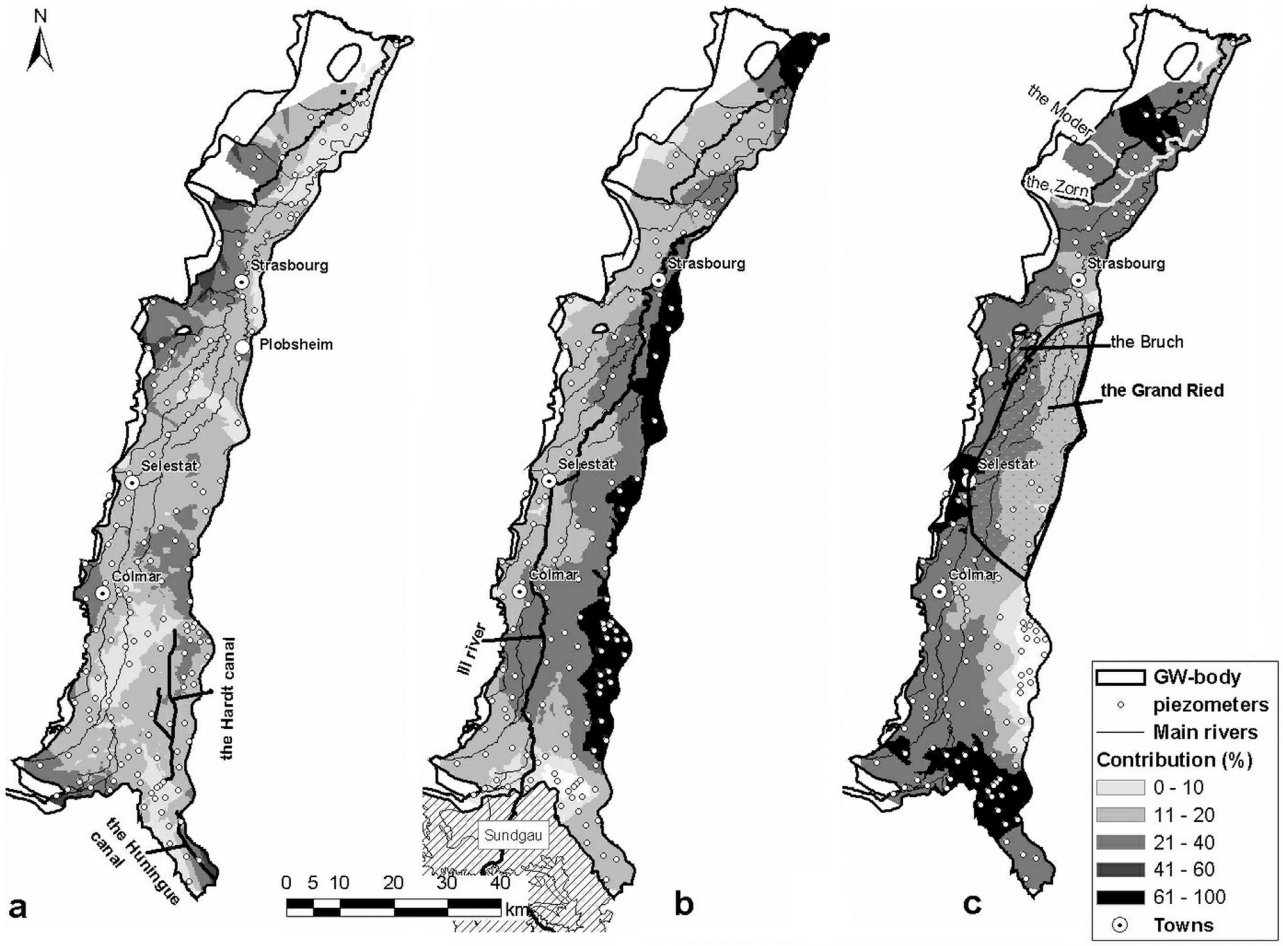

Figure 12. Mean contribution of rainfall and the surface water network to the Alsace aquifer from the inverse modeling of groundwater. Kriging is carried out with a cubic ordinary variogram. (a) Rainfall. (b) Rhine. (c) Vosgian rivers.

where ΔH_{obs} and ΔH_{mod} represent the observed and the modeled pressure head variations, both being centered, which is the ratio of the moments of inertia of the cloud (ΔH_{obs}, ΔH_{mod}) in relation to the first and the second bisectors (the center of gravity of the cloud is the origin of coordinates). The poorest correlations between the observed and the modeled pressure heads are reached at the north of Strasbourg and at the southern part of the Alsace water table, disclosing spatial patterns. At the south, bad correlations occur on the side of the Hardt canal opposite to the Rhine, where the Rhine contribution is still high and strongly delayed while the Rhine signal is blurred by the Hardt canal used for irrigation. At the north of Strasbourg, bad correlations are observed where the recharge from rainfall is significant while the response time of the water table is delayed, due to the low transmissivity of the vadose zone.

4. Analysis and Discussion

4.1. Contribution of the Rhine

[41] The main contributions of the Rhine associated with a short response time of less than 50 days are concentrated along the Rhine. They reveal the principal zones of exchange between the Rhine and the aquifer. Groundwater pressure head variations are concomitant with Rhine flow variations at the sampling rate scale, i.e., 15 days, near the port of Strasbourg, where wet docks help maintain the groundwater level, and south of Colmar. The main contributions of the Rhine associated with long response times (more than 50 days) reveal areas where the Rhine recharges the aquifer when the groundwater level is low. These are the Plobsheim region and the strip of land between the Hardt canal and the Rhine. The area south and north of Colmar where the Ill infiltrates also contributes significantly to maintaining the groundwater level when it is low. Exchanges between the Rhine and the aquifer are limited at the southern end of the Alsace plain where the vadose zone is over 20 m thick. The influence of the Rhine on groundwater decreases as we move toward the Vosges where the influence of Vosgian rivers increases. One exception is observed south of Colmar where the Rhine contribution is nearly 50%, probably because the Huningue canal, which is connected to the Rhine, flows into the Ill in summer.

4.2. Contribution of Vosgian Rivers

[42] The most highly influenced regions are located in the foothills of the Vosges and along the Ill River. South of

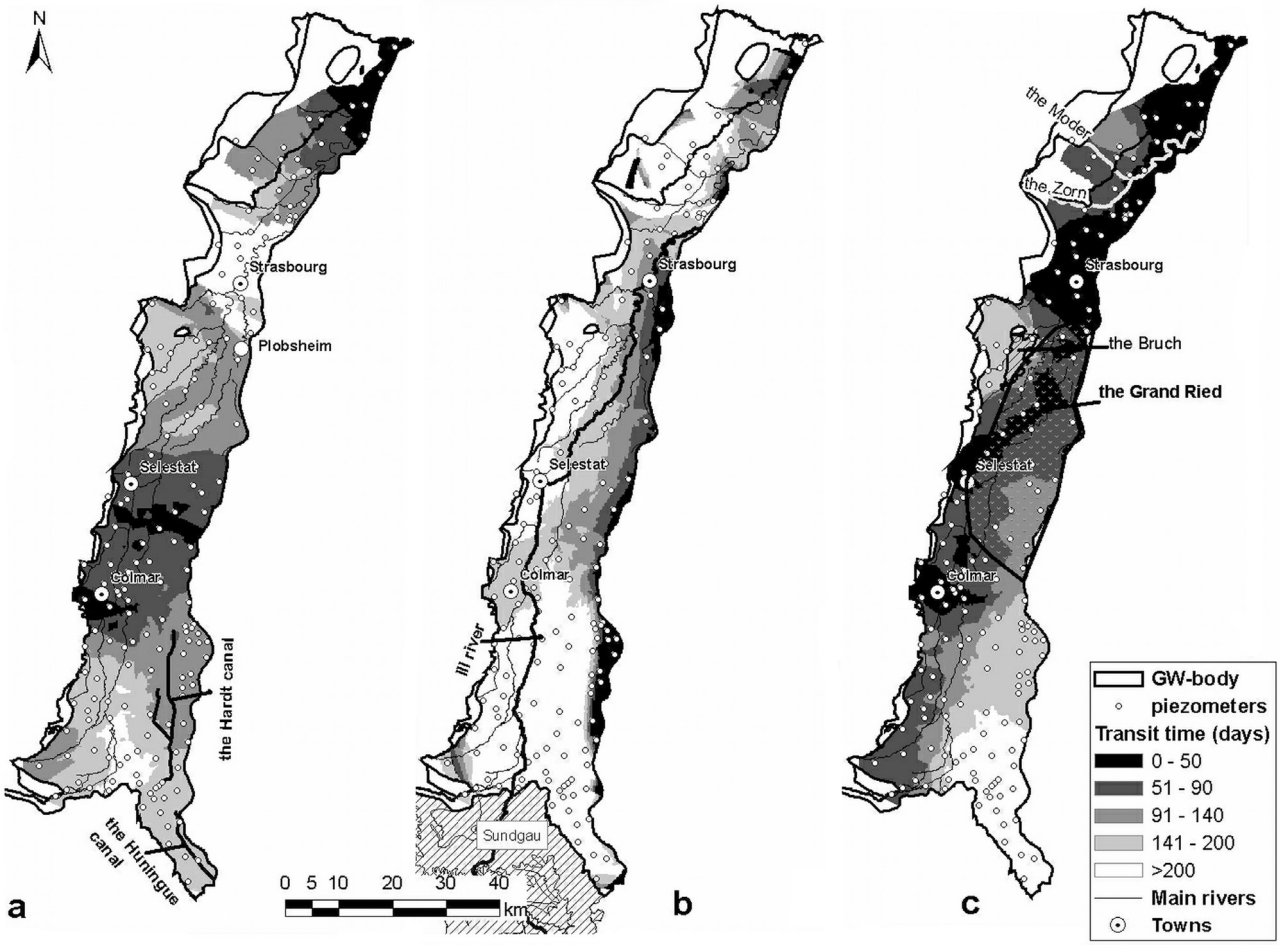

Figure 13. Mean response times of rainfall and surface water to the Alsace aquifer. Kriging is carried out with the same conditions as in Figure 12. (a) Rainfall. (b) Rhine. (c) Vosgian rivers.

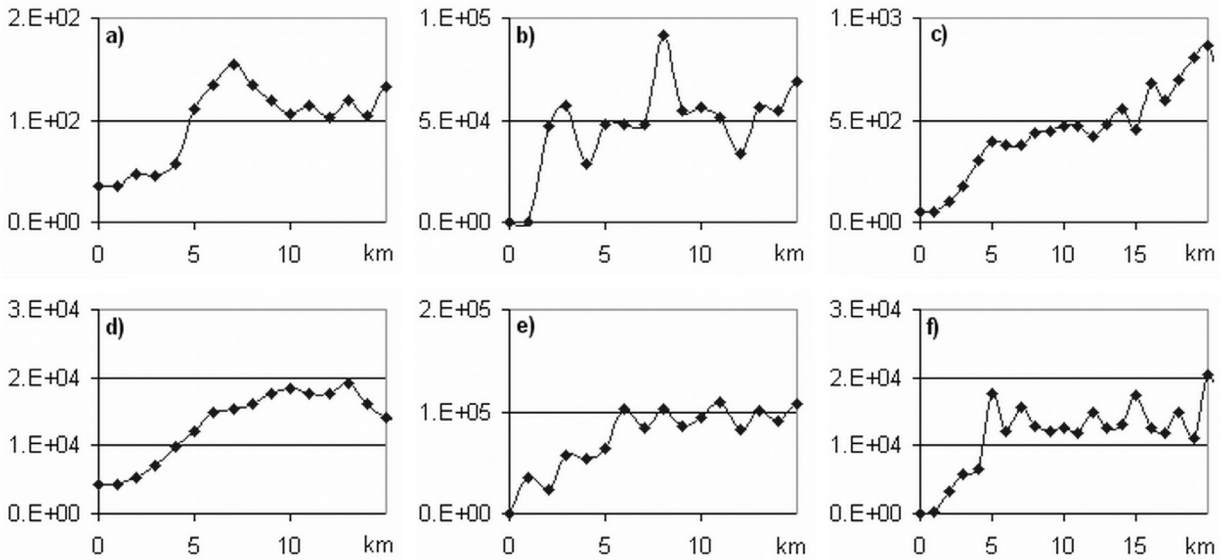

Figure 14. Mean variograms of the contribution to the recharge of (a) the rainfall, (b) the Rhine, and (c) the Vosgian drainages, and mean variograms of the response time of the water table to (d) the rainfall, (e) the Rhine, (f) the Vosgian drainages.

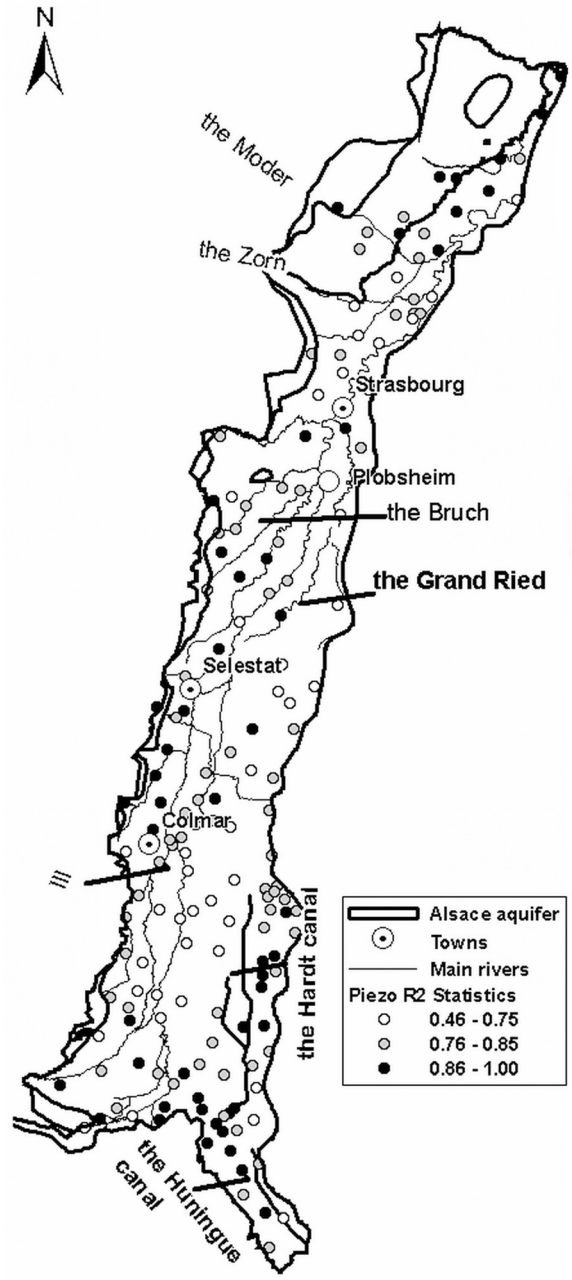

Figure 15. Representation of R^2 to quantify the goodness of fit of the pressure head.

Strasbourg, the Plobsheim water body (river lake) maintains the balance between the groundwater level and that of the Rhine. The influence of Vosgian rivers on groundwater decreases as we move toward the Rhine, apart from areas where there is a significant anthropic impact. In particular, the Hardt canal is filled in summer in order to maintain the groundwater level for irrigation. This may introduce confusion between the contribution of the Vosgian rivers and the Rhine in the transfer model, as it is reflected by the low value of the correlation coefficient R^2 in Figure 15.

[43] The Vosgian rivers influence two zones in particular: the northern and southern ends of the aquifer. In the north, where the hydrographic network is dense, more than half of the amplitude of the piezometric variations is attributed to exchanges between groundwater and Vosgian rivers. Response times are short, which indicates the high transmissivity of the aquifer formation and significant leakage from the hydrographic network. On the other hand, at the southern end of the aquifer, response times between the hydrographic network and the groundwater are long, more than 1 year where the vadose zone is more than 20 m thick. This indicates a low transmissivity of the vadose zone and aquifer. The Sundgau, which drains a multitude of small catchments, also recharges this area.

4.3. Contribution of Rainfall

[44] Effective rainfall contributes little to the piezometric variations (Figure 12a). Its contribution exceeds 30% only on the northern part at the foothills of the Vosges where the hydrographical network is sparse, and 20% to the east of a Colmar-Sélestat line where the vadose zone is less than 3 m thick (Figure 16). Reciprocally, it is low wherever the hydrographical network is dense because the soils have low permeability, which is favorable to the formation of wetlands. Infiltration is low south of Colmar where the vadose zone is over 10 m thick. The wetlands (the Grand Ried between Selestat and Strasbourg, the Bruch of the Andlau, the Zorn and the Moder) respond rapidly to precipitation due to the thinness of the vadose zone. South of Selestat, therefore, the response time of nearly 1 m per 10 days accurately reflects the thickness of the vadose zone at the regional scale (Figure 16). This shows that the permeability of the vadose zone is relatively homogeneous, apart from localized places. This strong similitude also appears at the northern end of the Alsace plain where the vadose zone is less than 2 m thick. On the other hand, the comparison of Figure 16a and 16b shows that the response of groundwater to rainfall is strongly delayed in the neighborhood of Strasbourg where the loess terraces are 5–10 m thick, the response time being 1 m per 50 days in some places. The great differences in vadose zone permeability reflect the contours and thickness of the terraces. More generally, the comparison of Figure 16a and 16b shows up the extension of loess plates in the northern half part of the Alsace plain.

5. Conclusion

[45] Separation of pressure head variations in the Alsace aquifer into three components related to rainfall, Vosgian rivers, and the Rhine greatly increases our understanding of recharge mechanisms and exchanges with the surface water network of this major groundwater system at the regional scale. In particular, several zones of the aquifer are shown to be strongly influenced by the hydrographical network where response times are short. Although the direct influence of the Rhine is limited to its immediate surroundings, it contributes to maintaining the level of the Alsace aquifer as a whole. This is significant when groundwater levels are low due to the long response times of more than 100 days. Direct recharge of groundwater by precipitation occurs only where the vadoze zone is thin. Rainfall does not significantly influence the groundwater level south of Colmar or in the northern part of the aquifer where soils are relatively impermeable. The mean response time of rainfall closely reflects the thickness of the vadose zone south of Selestat

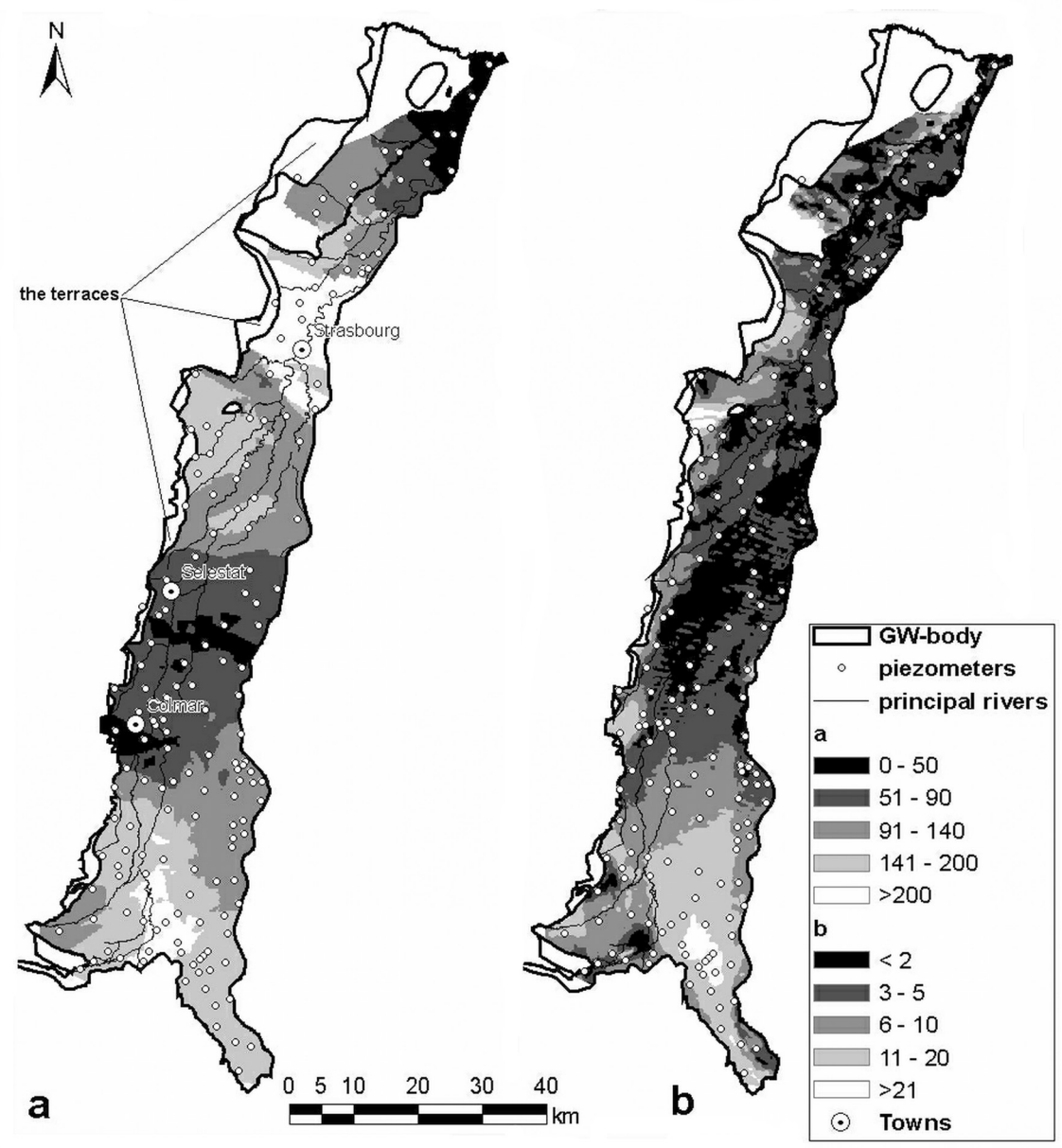

Figure 16. (a) The response time (days) in the vadose zone compared with (b) the thickness (meters) of the low-water vadose zone (APRONA, from regional hydrodynamic model data).

and at the northern end of the Alsace plain, whereas it discloses the contours and the thickness of the loess terraces nearby and south of Strasbourg to Selestat.

[46] **Acknowledgments.** This work was supported by the BRGM's research grant, the APRONA, and the Direction Régionale de l'Environment d'Alsace, France. We appreciate the contribution of the two anonymous reviewers as well as the associate editor, who significantly improved the understanding of the paper.

References

Carbiener, R. (1983), Le grand Ried d'Alsace: Ecologie et évolution d'une zone humide d'origine fluviale rhénane, *Bull. Ecol.*, *14*, 249–277.

Carrera, J. (1987), State of the art of the inverse problem applied to the flow and solute transport equations, in *Groundwater Flow and Quality Modeling*, *Math. Phys. Sci. Ser.*, vol. 224, edited by E. Custodio et al., pp. 549–583, D. Springer, New York.

Carrera, J., and S. P. Neuman (1986), Estimation of aquifer parameters under transient and steady state conditions: 1. Maximum likelihood method incorporating prior information, *Water Resour. Res.*, *22*(2), 199–210.

Cooley, R. L., L. F. Konikow, and R. L. Naff (1986), Nonlinear-regression groundwater flow modeling of a deep regional aquifer system, *Water Resour. Res.*, *22*(13), 1759–1778.

Ginn, T. R., and J. H. Cushman (1990), Inverse methods of subsurface flow: A critical review of stochastic techniques, *Stochast. Hydrol. Hydraul.*, *4*, 1–26.

Kaden, U. (1994), Etude de la séparation des écoulements sur différents bassins d'Alsace: Application et automatisation de la technique du base flow index (BFI), M.S. thesis, 55 pp., Univ. Louis Pasteur, Strasbourg, France.

Kitanidis, P. K. (1995), Quasilinear geostatistical theory for inversing, *Water Resour. Res.*, *31*(10), 2411–2419.

Kitanidis, P. K. (1999), Geostatistics: Interpolation and inverse problems, in *The Handbook of Groundwater Engineering*, edited by J. W. Delleur, pp. 12.1–12.20, CRC Press, Boca Raton, Fla.

Lavenue, A. M., B. S. Ramarao, G. de Marsily, and M. G. Marietta (1995), Pilot point methodology for automated calibration of an ensemble of conditionally simulated transmissivity fields: 2. Application, *Water Resour. Res.*, *31*(3), 495–516.

McLaughlin, D., and L. R. Townley (1996), A reassessment of the groundwater inverse problem, *Water Resour. Res.*, *32*(5), 1131–1162.

Pinault, J.-L. (2001), Manuel utilisateur de TEMPO: Logiciel de traitement et de modélisation des séries temporelles en hydrogéologie et en hydrogéochimie, *Rep. BRGM/RP-51459 –FR*, 233 pp., Project Modhydro, Bur. de Rech. Geol. et. Miner., Orleans, France.

Pinault, J.-L., H. Pauwels, and C. Cann (2001a), Inverse modeling of the hydrological and the hydrochemical behavior of hydrosystems: Application to nitrate transport and denitrification, *Water Resour. Res.*, *37*(8), 2179–2190.

Pinault, J.-L., V. Plagnes, L. Aquilina, and M. Bakalowicz (2001b), Inverse modeling of the hydrological and the hydrochemical behavior of hydrosystems: Characterization of karst system functioning, *Water Resour. Res.*, *37*(8), 2191–2204.

Pinault, J.-L., N. Doerfliger, B. Ladouche, and M. Bakalowicz (2004), Characterizing a coastal karst aquifer using an inverse modeling approach: The saline springs of Thau, southern France, *Water Resour. Res.*, *40*, W08501, doi:10.1029/2003WR002553.

Pinault, J.-L., N. Amraoui, and C. Golaz (2005), Groundwater-induced flooding in macropore-dominated hydrological system in the context of climate changes, *Water Resour. Res.*, *41*, W05001, doi:10.1029/2004WR003169.

Ramarao, B. S., A. M. Lavenue, G. de Marsilly, and M. G. Marietta (1995), Pilot point methodology for automated calibration of an ensemble of conditionally simulated transmissivity fields: 1. Theory and computational experiments, *Water Resour. Res.*, *31*(3), 475–493.

Sánchez-Pérez, J. M., and M. Trémolières (2003), Change in groundwater chemistry as a consequence of suppression of floods: The case of the Rhine floodplain, *J. Hydrol.*, *270*, 89–104.

Schmitt, L. (2001), Typologie hydro-géomorphologique fonctionnelle de cours d'eau: Recherche méthodologique appliquée aux systèmes fluviaux d'Alsace, Ph.D. thesis, 217 pp., Univ. Louis Pasteur, Strasbourg, France.

Sun, N. Z. (1994), *Inverse Problems in Groundwater Modeling*, Springer, New York.

Trémolières, M., I. Eglin, U. Roeck, and R. Carbiener (1993), The exchange process between river and groundwater on the central Alsace floodplain (eastern France): I. The case of the canalised River Rhine, *Hydrobiologia*, *254*, 133–148.

Trémolières, M., U. Roeck, J. Klein, and R. Carbiener (1994), The exchange process between river and groundwater on the central Alsace floodplain (eastern France): II. The case of a river with functional floodplain, *Hydrobiologia*, *273*, 19–36.

Trémolières, M., R. Carbiener, I. Eglin, F. Robach, U. Roeck, and J. M. Sánchez-Pérez (1997), Surface water/groundwater/forest alluvial ecosystems: Functioning of interfaces—The case of the Rhine floodplain in Alsace (France), in *Groundwater-Surface Water Ecotones: Biological and Hydrological Interactions and Management Options*, edited by J. Gilbert et al., pp. 91–101, Cambridge Univ. Press, New York.

Yeh, W. W.-G. (1986), Review of parameter identification procedures in groundwater hydrology: The inverse problem, *Water Resour. Res.*, *22*(2), 95–108.

J.-L. Pinault, Water Research Division, Bureau de Recherches Géologiques et Minières, 3 avenue Claude Guillemin, 45060 Orléans, France. (jl.pinault@brgm.fr)

S. Schomburgk, Parc Club des Tanneries, Bureau de Recherches Géologiques et Minières, 15 rue du Tanin, Lingolsheim, BP 177, 67834 Tanneries Cedex, France.